Article citation info:
Sawczuk W, Rilo Cañás AM, Kołodziejski S. Thermal imaging of the disc brake and drive train in an electric locomotive in field conditions. Combustion Engines. 2024;196(1):161-168. https://doi.org/10.19206/CE-174320

Wojciech SAWCZUK
Armando Miguel RILO CAÑÁS
Sławomir KOŁODZIEJSKI

Combustion Engines
Polish Scientific Society of Combustion Engines

Thermal imaging of the disc brake and drive train in an electric locomotive in field conditions

ARTICLE INFO

Received: 28 July 2023
Revised: 22 September 2023
Accepted: 19 October 2023
Available online: 25 November 2023

The article presents the results of thermovision tests of the disc brake and the drive system components located in its vicinity on the 111Ed electric locomotive in field conditions. For this locomotive, tests were carried out on a test track to measure the temperature of the disc and the temperature of other devices that were installed close to the brake disc. These tests were performed pointwise, i.e. before and after the test, and continuously throughout the braking process. The article presents the methodology of thermal imaging research and the preparation of the camera for outdoor research with objects with different emissivity. Due to the rotating brake disc, it was decided to measure using an IR camera because measurements using thermocouples were very difficult and complex. In exceptional situations, temperature measurement using thermocouples is used, but it requires an extensive additional measurement system and signal recording, which is more expensive. Correct configuration of the IR camera to real conditions is extremely important because it directly translates into the increase in measurement error.

Key words: *thermal imaging, emissivity, disc brake, electric locomotive, drive train system*

1. Introduction

The thermal imaging camera enables indirect measurement (non-contact at a distance) by recording in the lens the infrared radiation emitted by the tested element in the electromagnetic wavelength range. Each body that has a temperature higher than absolute zero, i.e. 0 K, emits energy in the form of infrared radiation, however, it should be noted that the radiation energy coming from the tested element depends on the length of the electromagnetic wave and the temperature of this object [2, 4, 6]. The IR camera has a built-in infrared detector to convert the energy coming from incident infrared photons from the tested device (element) into an electrical signal. The value of this signal is directly proportional to the temperature of the tested object [3, 12]. Electrical signals in the form of color images are converted into thermograms. This is due to the fact that the tested objects emit radiation of a certain power, which is called luminance. Different intensities of infrared radiation translate into the temperature distribution visible in the thermal image (thermogram).

Fig. 1. View and construction of the FLIR e60 thermal imaging card used in later studies: 1 – lens, 2 – control buttons, 3 – trigger, 4 – camera handle, 5 – laser, 6 – display [11]

The general structure of a thermal imaging camera is shown in Fig. 1. The cameras can be used as portable devices with a handle under the operator's hand (inspection cameras) or as research cameras mounted on a tripod [15].

The division of cameras is diverse. Inspection and research cameras were mentioned earlier, but IR cameras are also divided into devices only for observing objects and related temperature distribution and cameras for simultaneous observation and measurement of temperature values. Detectors that are built into cameras as measurement transducers determine their further division. It should be noted that bolometric cameras are most often used due to the widest range of recorded infrared wavelengths [6, 18]. These types of cameras are used in construction, the power industry or testing machines, and internal combustion engines, as presented in [16, 19].

2. Emissivity determination methods

The thermal imaging camera requires configuration of settings to the conditions that prevail during the tests. Particular attention should be paid to the emissivity (ε factor) setting. The other parameters set in the IR camera, besides emissivity, are ambient temperature, air humidity, and reflected temperature. These parameters, if entered incorrectly during configuration, cause a slight increase in the measurement error by approximately 1–2°C [8]. The emissivity recorded in the camera has the greatest impact on the measurement error (several dozen percent). This is a parameter related to the ability of the tested body to emit real radiation related to the emission from a black body.

$$\varepsilon = \frac{W_{CR}}{W_{DC}} \tag{1}$$

where: W_{DC} – black body radiation, W_{CR} – real body radiation.

It is also defined as the ratio of the intensity of real radiation to the infrared radiation of a black body at the same

temperature as the tested object and the perfect black body, which shows the relationship (1) [9].

The value of the coefficient depends on such factors as the type of body, its temperature, the wavelength of the radiation as well as the condition of the surface [12]. Depending on the surface (polished or rough), the emissivity coefficient may vary from 0.1 to 0.98. Test objects with polished surfaces have an emissivity coefficient even below 0.1 because they reflect approximately 99% of external radiation. All infrared radiation does not reach the camera lens. Rough and black surfaces mean that all the radiation reaches the IR camera lens (ε above 0.9) [2].

There are three ways to determine the emissivity in thermal imaging. It is a calorimetric, reflection and reference body method. The emissivity coefficient in the calorimetric method can be calculated using two methods.

The first method involves using a camera that measures spectral existence. Emissivity is determined by measuring the temperature from a thermocouple. The second method is based on the calculation of spectral existence based on relation (2) [10].

$$M(T) = \varepsilon M_c(T_o) + (1 - \varepsilon)M_\alpha(T_\alpha) \quad (2)$$

where: $Mc(T_o)$ – the existence of a blackbody at the temperature of the object T_o, $M\alpha(T_\alpha)$ – background existences about temperature T_α.

On the basis of the Stefan-Boltzmann law, it is possible to determine the value of existence knowing the temperatures of the object T_o and the ambient (background) temperature T_α, respectively [6]. Then the actual emissivity coefficient is calculated based on equation (3) [9].

$$\varepsilon = \frac{T^4 - T_\alpha^4}{T_o^4 - T_\alpha^4} \quad (3)$$

where: T – temperature value when ε = 1.

The reflection method uses two heat sources, i.e. Z1 and Z2, whose temperatures are different. The following radiation then reaches the camera lens:

- two heat sources Z_1 and Z_2
- reflected from the tested object $(1 - \varepsilon)M_{Z1}$ or $(1 - \varepsilon)M_{Z2}$
- reflected from the mirror M_{Z1} or M_{Z2}
- own properties of the tested object $\varepsilon Mc(T_0)$.

In the reflection method, the emissivity coefficient is calculated based on equation (4) [11]:

$$\varepsilon - 1 = \frac{M_1 - M_2}{M_{Z1} - M_{Z2}} \quad (4)$$

where: M_1, M_2 – existence of the test body illuminated by the source Z_1 and Z_2, M_{Z1}, M_{Z2} – existence of the first and second light sources.

The method with a reference body requires the use of two objects, one of which has a known emissivity ε_r. Both objects, i.e. the tested and reference objects, are located next to each other so that the impact of the environment is the same. This will make the temperature T0 for both objects the same. The next step is to determine the existence of both objects. The actual emissivity of the tested object is calculated in equation (5) [10].

$$\varepsilon = \varepsilon_r \frac{M_1 - M_\alpha}{M_2 - M_\alpha} \quad (5)$$

where: M_1, M_2 – the existence of the test body and the reference one, M_α – ambient radiation energy using a mirror covering the object and with a reflection coefficient of ρ = 1 [9], ε_r – emissivity of the reference body.

In the practice of thermal imaging measurements of mechanical objects, the calorimetric method is most often used. People measuring with an IR camera use thermocouples anyway when configuring the camera, which is carried out so long that the temperature from the thermocouple and the IR camera is the same. In this method, special attention should be paid to the background temperature [11]. However, in thermal imaging measurements in buildings and engineering structures, the method with a reference body is a popular method. Method with a reference body is similar to the calorimetric method because two measurements are performed simultaneously, i.e. a reference and a real object. In the camera settings, the emissivity value is changed for such a long time to obtain the same temperature values in the examined objects [8].

3. Research methodology

3.1. Purpose and object of thermovision research

The aim of the tests was to determine the temperature distribution of the brake disc and elements in its surroundings during braking on the 111Ed-004 electric locomotive (Fig. 2) for compliance with the requirements of UIC and TSI Loc&Pas [1, 7]. The locomotive is equipped with a friction disc brake [17].

Fig. 2. View of the electric locomotive 111Ed-004 on the experimental track in Żmigród

The object of the tests was the Knorr-Bremse (KB) disc brake assembly located on the bogie of the electric locomotive (Fig. 3a and 3b) and the drive system components located in its vicinity [3, 16, 20].

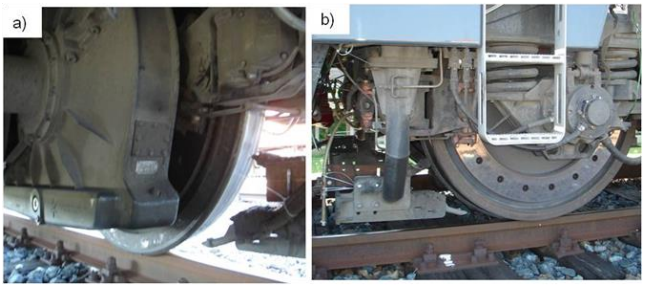

Fig. 3. Object of thermal imaging tests: a) view of the disc braking system and drive gear from the locomotive chassis, b) view of the braking mechanism outside the locomotive

In addition, after a series of emergency and service braking, the temperature increments of the components located in the immediate vicinity of the brake disc, such as the drive gear, springs of the first degree of suspension, the bogie frame, the bearing housing and the rim of the railway wheel, were determined [10]. The influence of the temperature increase (local overheating) on the increase in stresses in the material and its deformations is described in more detail in [1, 14]. The temperature values of the mentioned elements were referred to the initial state before starting the temperature tests.

3.2. Research method

The tests of the temperature distribution of the brake disc were carried out using a FLIR e60 microbolometer camera. The tests were carried out in field conditions on the test track of the Railway Institute in Żmigród.

The thermovision tests were preceded by the initial configuration of the camera settings to the conditions that occurred during the test on the locomotive chassis. The parameters necessary to make settings in the IR camera are air temperature, reflected temperature, humidity, and distance from the tested object. The camera was mounted in a housing attached to the opposite side of the tested brake disc, with elements located in its immediate vicinity, as shown in Fig. 4.

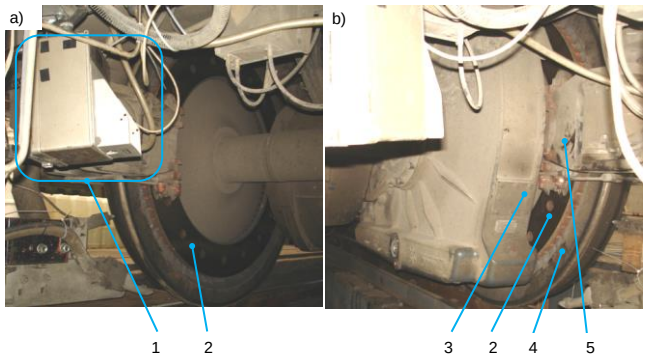

Fig. 4. View from the locomotive chassis with the tested objects: a) view of the housing with a thermal imaging camera mounted (1) at the left wheel of the wheelset, b) view of the tested elements with a thermal imaging camera: 2 – brake disc, 3 – drive gear housing, 4 – drive wheel rim, 5 – disc brake caliper

In the process of configuring the camera for the conditions that existed before the tests, special attention was paid to determining the emissivity coefficient ε.

In the case of testing the temperature distribution of the elements around the brake disc, as shown in Fig. 3b, it was possible to determine one common value of the coefficient ε. These elements are characterized by low reflectivity due to the rough and dark surface, which translates into a high value of the emissivity coefficient. However, in the case of the brake disc itself with a luminous (polished) friction surface characterized by high reflectivity (reflection coefficient), a low value of the emissivity coefficient is introduced. During thermal imaging studies of objects characterized by high reflectivity, using the calorimetric method described in [2, 6], it was possible to determine the actual emissivity coefficient. However, in the case of testing the temperature distribution of rail vehicle components during braking, characterized by different values of the emissivity coefficient, it was necessary to assume one value of the ε coefficient as for most low-reflectivity components, and in the case of a highly reflective object, such as a brake disc, it is necessary to determine correction factors. For this purpose, the method of comparing the temperature result obtained from the thermal imaging camera with the result obtained from the sheathed thermocouple is used. Figure 5 shows the view of temperature measurement from the brake disc with a sheathed thermocouple in order to determine the correction factor. The same method was used to determine the actual temperature values of vehicle components located in the vicinity of the brake disc. The next step in configuring the thermal imaging camera was to gradually change the emissivity coefficient value to obtain the same temperature value read from the IR camera and from the thermocouple.

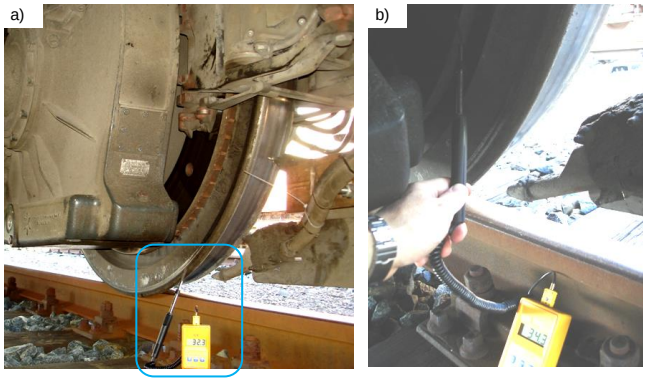

Fig. 5. View of the GTH 1179 temperature sensor with a sheathed probe when measuring the actual temperature of: a) railway wheel, b) brake disc

In the case of testing the temperature distribution on such locomotive elements as the frame, the housing of wheel set bearings, and springs of the first degree of suspension, a thermovision measurement was carried out before the test and after a series of emergency and service braking from the set braking speeds of the locomotive. Figure 5 shows the view of the tested vehicle elements located in the vicinity of the brake discs. The thermal images recorded using a thermal imaging camera were then analyzed in the FLIR Tools program. Figure 6 shows an example thermogram of a disc from a brake disc with measuring points Sp1, Sp2 and Sp3 inserted. These points made it possible to measure the temperature values on three radii of the brake disc. This was necessary to determine the correction factor to calculate the actual brake disc temperature.

Then, according to the relationship (6), the correction factor was determined based on [2] the thermovision measurement in relation to the measurement using a thermocouple.

$$K_{(\dots)} = \frac{T_{TC}}{T_{IR}} \tag{6}$$

where: T_{TC} – temperature value in °C obtained when measured with a sheathed thermocouple, T_{IR} – temperature value in °C obtained when measuring with a thermal imaging camera.

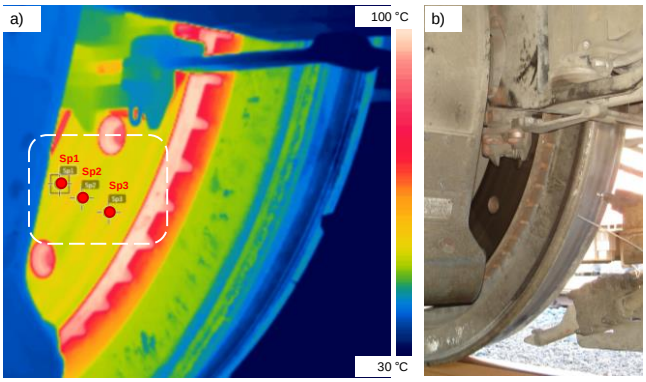

Fig. 6. a) image from a thermal imaging camera of a wheel with a brake disc with measuring points Sp1, Sp2 and Sp3, b) view from the locomotive chassis of a fragment of a wheel with a brake disc in the process of configuring the thermal imaging camera for testing

Then, the actual temperature value of the tested element using the non-contact method using a thermal imaging camera during the locomotive braking was determined in accordance with the following relationship (7):

$$T_{rz\,(\ldots)} = K_{(\ldots)} \cdot T_{IR} \tag{7}$$

where: $T_{rz(\ldots)}$ – the actual value of the temperature of the disc in °C or of the tested locomotive element located in the vicinity of the brake disc.

On the basis of dependencies (6) and (7), correction factors were determined (Table 1) for testing the temperature distribution on the brake disc in motion and on such elements in its vicinity as the brake caliper, wheel and gear housing.

Table 1. Values of correction factors in temperature tests

Tested object	Temperature in °C		Correction factor
	Thermocouple measurement	Measurement with an IR camera	
Brake disc	205.0	90.0	2.278
Wheel	52.0	51.0	1.019
Brake caliper	39.8	35.6	1.118
Drive gear	41.7	41.0	1.017

Table 2. Parameter values of the thermal imaging camera configured for the purpose of testing the temperature distribution of the brake and elements in its surroundings

No.	Parameter	Value
1	Emissivity for objects in the vicinity of the brake disc	0.97
2	Emissivity for the brake disc	0.31
3	Reflected apparent temperature	31°C
4	Distance	1 m
5	Relative humidity	50%
6	Air temperature	31°C
7	External optics temperature	20°C
8	Transmission of the external optical system	1.0

Based on the evaluation of the temperature values determined by the contact and non-contact methods, the actual emissivity coefficients were determined, which, together with the other parameters for the camera configuration, are included in Table 2. Temperature changes in the tested objects on the locomotive chassis were observed from the driver's cab using a Video Grabber converter connected to a camera located under the vehicle. Real-time observation was possible using the Visual Studio 10 software installed on the laptop and a long cable connecting the camera to the laptop via the USB port. The converter allowed for recording analog signals from the camera into digital form on the laptop's hard drive.

4. The course and results of thermal imaging tests

Due to the mounting of the thermal imaging camera on the locomotive chassis, it was not possible to measure the temperature on such elements as the bogie frame, wheel set bearing housings or first-stage springs. Mounting the camera outside the vehicle was not possible due to exceeding the rolling stock gauge. Thermovision measurement of a larger number of elements involves moving the camera away from the tested objects by more than 1 meter so that the radiation emitted by the tested elements is concentrated in the optical system of the camera, and consequently in the camera detector. Therefore, the study of the temperature distribution on the locomotive chassis components was divided into a test in motion and a static test when the locomotive was stopped. The test in motion (during braking) included such elements as the brake disc, wheel, disc brake caliper and drive gear housing). The tangential test (at the moment of stopping the locomotive) was carried out on the frame, bearing housing, springs of the first spring rate, brake caliper and on the wheel (measurement on the wheel disc and wheel rim). Table 3 presents the results of temperature measurements of the disc and elements in its vicinity before the motion tests.

Table 3. Summary of temperature values before testing

Tested object	Wheel 1	Wheel 2
Brake disc	39.9	45.6
Axle bearing housing	37.3	42.6
Railway wheel wreath	40.0	44.7
Trolley frame	34.2	36.9
Ambient temperature T_o = 30.9°C		

Continuous thermovision images were recorded for sudden braking at speeds of v = 100, 120, 140 and 160 km/h. Selected images from the recording of the disc temperature distribution during braking from the speed of v = 160 km/h are shown in Fig. 7.

Example graphs of the peak values of the brake disc temperature recorded from the beginning of braking to stopping the electric locomotive during emergency braking from speeds of v = 120, 140 and 160 km/h as a function of braking time are shown in Fig. 8. The graphs were prepared on the basis of thermal images from a camera located on the locomotive chassis.

On the other hand, Fig. 9 shows the distribution of temperature on such elements located on the vehicle chassis as the housing of the wheel set drive gear, disc brake caliper and wheel rim from the inside during emergency braking from different speeds. The temperature values of the brake disc and other elements of the locomotive were corrected by the coefficient recorded in Table 1.

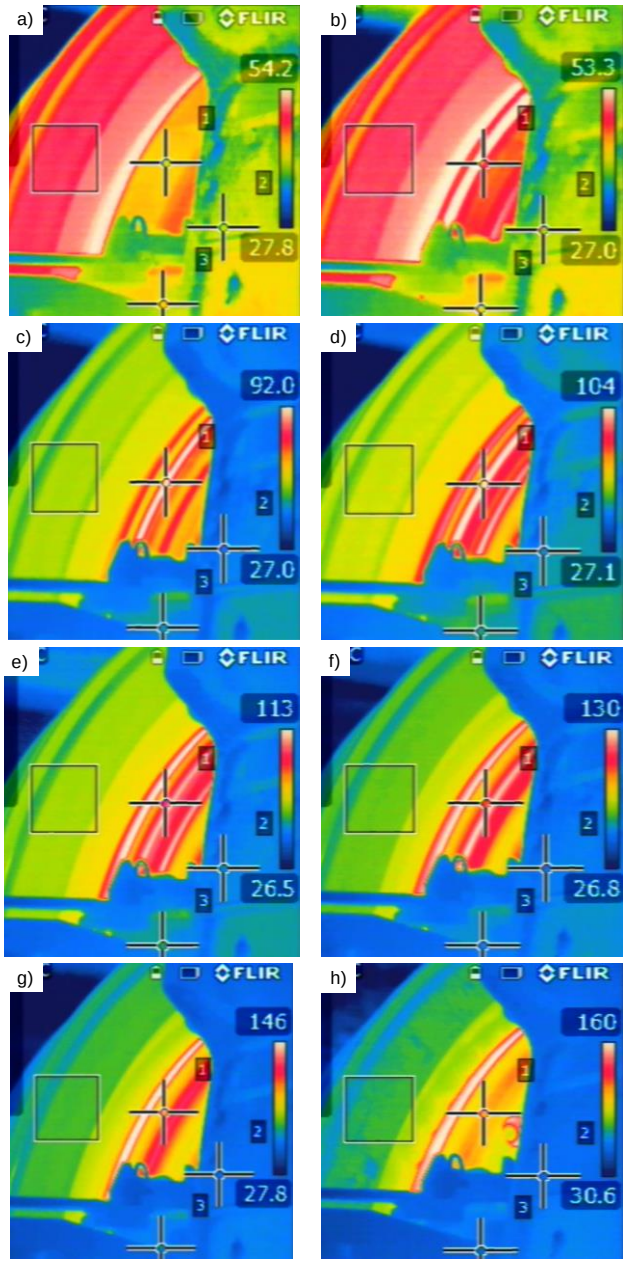

Fig. 7. Selected thermovision photos of the temperature distribution of the brake disc and its surroundings during emergency braking from a speed of 160 km/h; a) before braking, b) 5 seconds of braking, c) 8 seconds, d) 12 seconds, e) 18 seconds, f) 24 seconds, g) 34 seconds, h) stopping

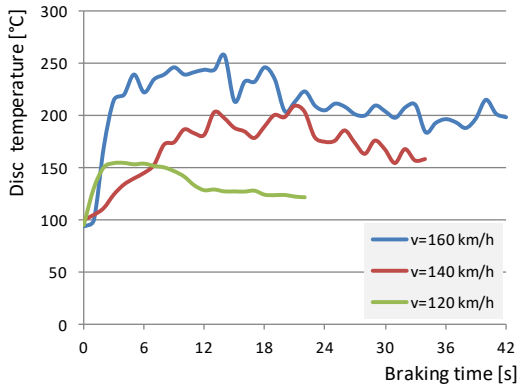

Fig. 8. Temperature distribution on the brake disc during braking from the speed of v = 120, 140 and 160 km/h, emergency (emergency) braking

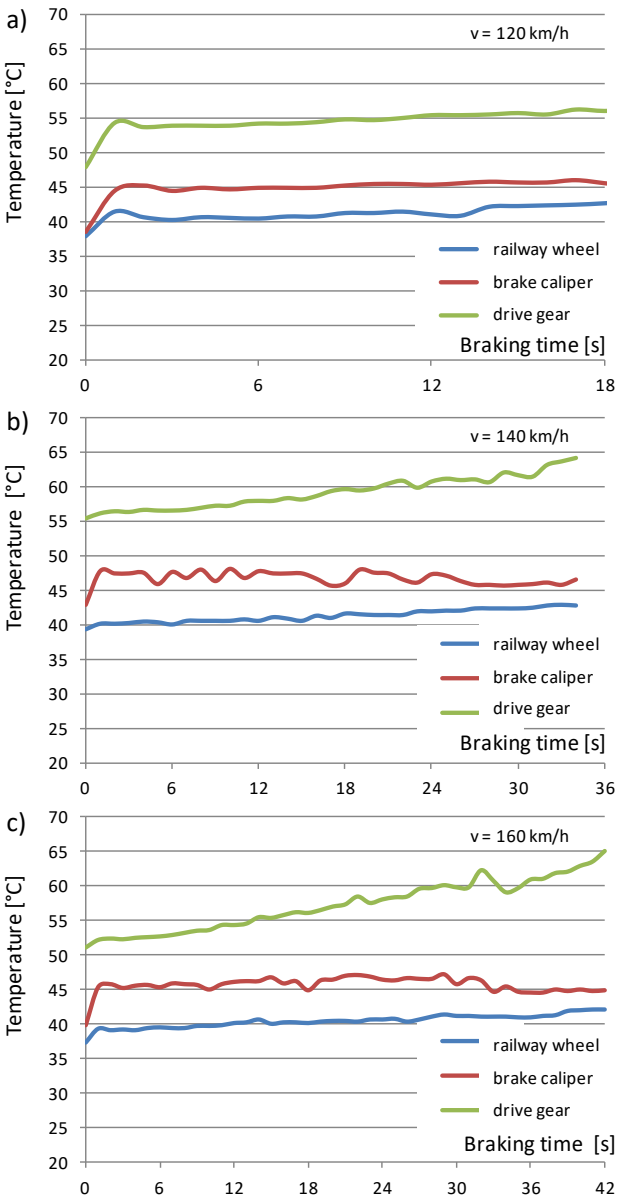

Fig. 9. Temperature distribution on the elements in the vicinity of the brake disc, i.e. the inner side of the wheel, the disc brake caliper and the wheel set drive gear, during braking from the speed of: a) v = 120 km/h, b) v = 140 km/h, c) v = 160 km/h, emergency braking

Figure 10 shows the peak values of the temperature of the disc (I) and the elements in its vicinity for several selected braking speeds (v = 140 and 160 km/h). The blue bars show the temperature before the tests, while the red bars show the temperature after the tests.

Figures 11, on the other hand, show an exemplary combination of both thermal and digital images with the temperature distribution of the disc and elements in its vicinity for one of the wheels of the locomotive. The measurement was carried out in two stages, i.e. before the start of the tests and after a series of 14 brakings.

Figure 12 shows the temperature distribution on the locomotive chassis in order to identify areas with the highest temperature in the vicinity of the brake disc.

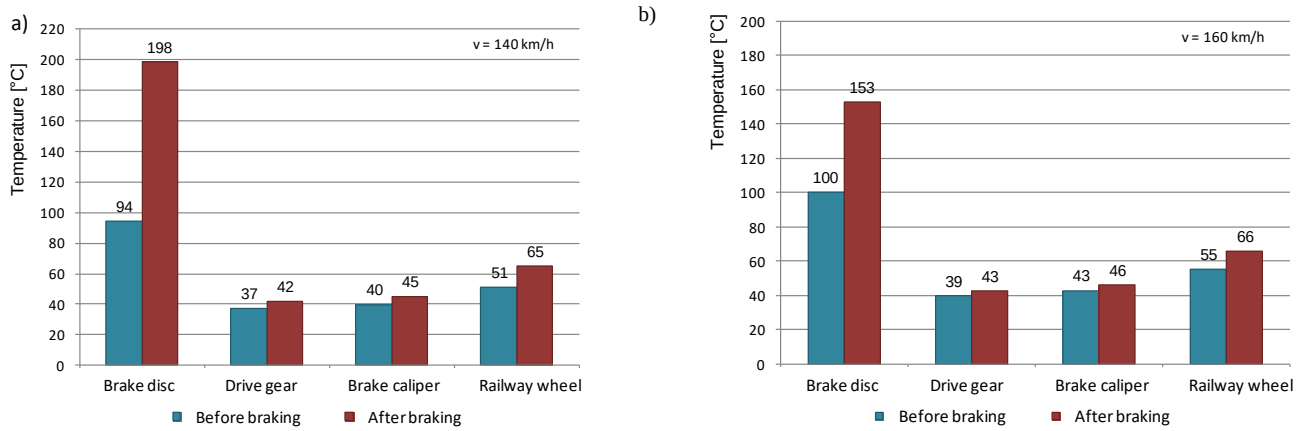

Fig. 10. Temperature increase of the brake disc and elements in its vicinity before and after braking from the speed of: a) v = 140 km/h, emergency braking, b) v = 160 km/h, emergency braking)

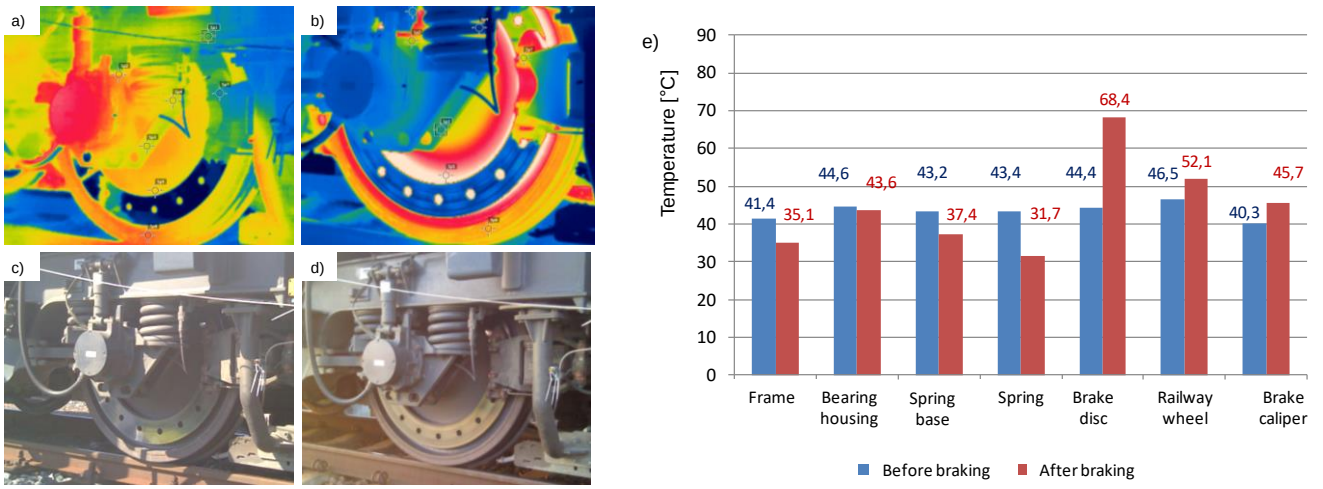

Fig. 11. Temperature distribution in the vicinity of wheel No. 1: a) IR photo before the tests, b) IR photo after the tests, c) digital photo before the tests, d) digital photo after the tests, e) diagram of the maximum temperature distribution of the brake disc and its components environment

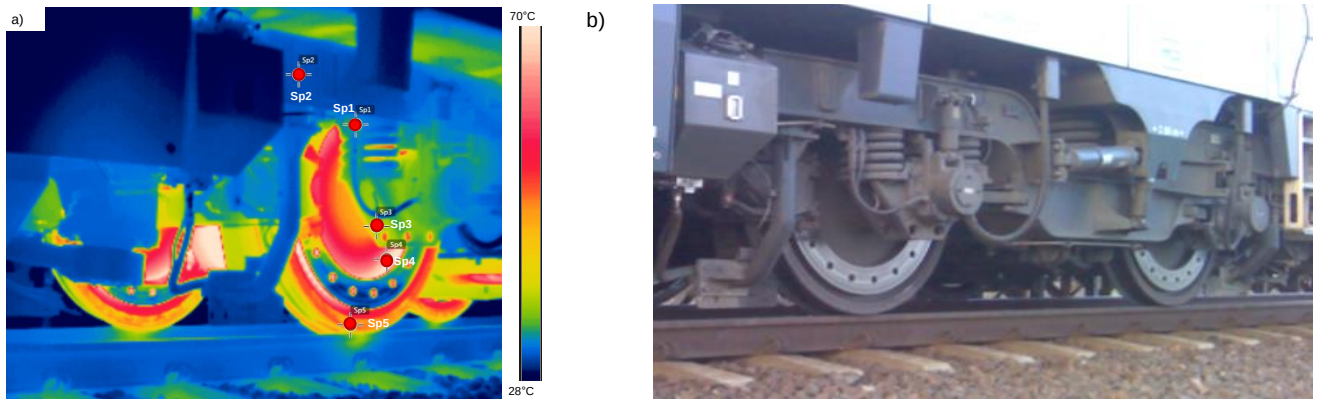

Fig. 12. Temperature distribution on the locomotive chassis after tests on the experimental track after a series of 14 brakings: a) IR photo after all tests, c) digital photo: Sp1 – bogie frame above the brake disc, Sp2 – bogie frame (string member), Sp3 – bearing housing base and springs, Sp4 – wheel disc, Sp5 – wheel rim

The final summary of the maximum values of the temperatures of the brake disc and its surroundings after a series of 14 brakings at various speeds is presented in Table 4. Static tests (vehicle stopped) were carried out in two stages, i.e. in pre-test conditions and also in fixed conditions after a series of braking.

Analyzing the obtained maximum values of the elements located in the immediate vicinity of the brake disc under the locomotive, it was found that the highest temperature increase was observed on the wheel disc (increase by about 33°C (306.15 K) compared to the state before the tests), wheel rim (increase by 15°C (288.15 K)), disc brake caliper (increase by about 34°C (307.15 K)) and the gear

housing of the wheelset drive – increase by 6°C (279.15 K). The brake disc, both during tests in motion and static at speeds of 100, 120, 140 and 160 km/h, does not exceed the value of 400°C (673.15 K) when braking on organic friction linings in accordance with the UIC 541-3 card.

Table 4. Summary of the maximum temperature values after the tests

Point designation	The name of the tested item	Temperature in [ºC]
Sp1	The frame of the trolley surrounded by the brake disc	34.7
Sp2	Bogie frame (string member) above the brake disc	31.3
Sp3	The base of the housing of bearings and springs	38.1
Sp4	Wheel disc	67.3
Sp5	Railway wheel wreath	51.6
Ambient temperature T_o = 26.0°C		

5. Conclusions

Based on the thermovision tests of the temperature distribution of the brake disc and its surroundings in real conditions on the chassis of the 111Ed locomotive, it was found:

a) that individual braking, both service and emergency, do not significantly affect the increase in temperature of components and devices located on the chassis of the tested locomotive. In the test of continuous recording of the temperature distribution with a thermal imaging camera, the maximum temperature increase after emergency braking from a speed of 160 km/h was 5°C (278.15 K) for the gear housing and brake caliper (increase by 12% compared to the temperature before braking) and 14.5°C (287.65 K) for the wheel rim of the wheelset (increase by 23%)
b) in the static test with the use of a thermal imaging camera, after recording the IR image of the locomotive chassis before and after braking, no temperature increases were found on such elements as the frame near the brake disc, springs of the first degree of springing or the housing of wheel set axle bearings (measurement at two points i.e. directly above the bearing and spring support housing). The temperature increase occurred only on the wheel disc, wheel rim and disc brake caliper. The maximum temperature increase values were 40°C (313.15 K) for the wheel disc, 18°C (291.15 K) for the wheel rim and 8°C (281.15 K) for the brake caliper. Under the locomotive, the temperature rise on the wheel was about 33°C (306.15 K), the wheel rim was 15°C (288.15 K), the disc brake caliper was 34°C (307.15 K) and the gear housing was 6°C (279.15 K)
c) the maximum permissible disc temperature was not exceeded after emergency and service braking according to card [1, 6]. Braking from a speed of 160 km/h increases the maximum disc temperature to about 260°C (533.15 K) during braking and about 200°C (473.15 K) when stopping.

Acknowledgements

The investigations were carried out within the Implementation Doctorate Program of the Ministry of Education and Science realized in the years 2021–2025.

Nomenclature

UIC	Union Internationale des Chemins de fer	Ed	electric locomotive with a diesel shunting engine
TSI	Technische Spezifikation für die Interoperabilität	KB	Knorr-Bremse brake system

Bibliography

[1] Czapp S, Szultka S, Ratkowski F, Tomaszewski A. Risk of power cables insulation failure due to the thermal effect of solar radiation. Eksploat Niezawodn. 2020;22(2):232-240. https://doi.org/10.17531/ein.2020.2.6
[2] Karabacak YE, Özmen NG, Gümüşel L. Worm gear condition monitoring and fault detection from thermal images via deep learning method. Eksploat Niezawodn. 2020;22(3): 544-556. https://doi.org/10.17531/ein.2020.3.18
[3] Matusiak K, Goliwąs D, Kaluba M. Adsorption dryer for use in railways. Rail Vehicles/Pojazdy Szynowe. 2022;(1-2):77-85. https://doi.org/10.53502/RAIL-152486
[4] Miao Z, Tu R, Kai Y, Huan G, Kang L, Zhou X. A novel method based on thermal image to predict the personal thermal comfort in the vehicle. Case Studies in Thermal Engineering. 2023;45:102952. https://doi.org/10.1016/j.csite.2023.102952
[5] Ortega-Farias S, Esteban-Condori W, Riveros-Burgos C, Fuentes-Peñailillo F, Bardeen M. Evaluation of a two-source patch model to estimate vineyard energy balance using high-resolution thermal images acquired by an unmanned aerial vehicle (UAV). Agr Forest Meteorol. 2021;304-305(15): 108433. https://doi.org/10.1016/j.agrformet.2021.108433
[6] Pathmanaban P, Gnanavel BK, Anandan SS. Comprehensive guava fruit data set: digital and thermal images for analysis and classification. Data in Brief. 2023;50:109486. https://doi.org/10.1016/j.dib.2023.109486
[7] Rooj S, Routray A, Mandal MK. Feature based analysis of thermal images for emotion recognition. Eng Appl Artif Intel. 2023;120:105809. https://doi.org/10.1016/j.engappai.2022.105809
[8] Ramani V, Martin M, Arjunan P, Chong A, Poolla K, Miller C. Longitudinal thermal imaging for scalable non-residential HVAC and occupant behaviour characterization. Energ Buildings. 2023;287:112997. https://doi.org/10.1016/j.enbuild.2023.112997
[9] Sawczuk W, Pagórek B. Compatibility of the λ-Kolmogorov test of the brake disc emissivity factor distribution in thermal imaging studies. Measurement Automation Monitoring. 2016;2:56-61.
[10] Sawczuk W, Rilo Cañás AM. The issues of hot-spots type in the railway disc brake. Rail Vehicles/Pojazdy Szynowe. 2021;1:33-43. https://doi.org/10.53502/RAIL-138492
[11] Sawczuk W, Rilo Cañás AM. Thermal imaging test of the disk brake of a diesel multiple unit in field conditions. Rail Vehicles/Pojazdy Szynowe. 2020;3:28-36. https://doi.org/10.53502/RAIL-138554

[12] Sangnoree A, Chamnongthai K. Thermal-image processing and statistical analysis for vehicle category in nighttime traffic. J Vis Commun Image R. 2017;48:88-109. https://doi.org/10.1016/j.jvcir.2017.06.006
[13] Song B, Park K, Kim SH, Park G. Comparison of an unmaned aerial vehicle based physical environment with thermal properties from in-situ measurements: Campus of Changwon National University, South Korea. Sustain Cities Soc. 2023;98:104836. https://doi.org/10.1016/j.scs.2023.104836
[14] Stoukatch S, Dupont F, Laurent P, Redouté JM. Package design thermal optimization for metal-oxide gas sensors by finite element modeling and infra-red imaging characterization. Materials. 2023;16(18):6202. https://doi.org/10.3390/ma16186202
[15] Sun H, Zhu HY, Han J, Fu Ch, Chen MM, Wang K. Energy and infrared radiation characteristics of the sandstone damage evolution process. Materials. 2023;16(12):4342. https://doi.org/10.3390/ma16124342
[16] Wu J, Liu J, Zhao J, Su Y. Influencing assessment of different heating modes on thermal comfort in electric vehicle cabin. Energy and Built Environment. 2023. https://doi.org/10.1016/j.enbenv.2023.04.005
[17] Zemlik M, Dziubek M, Pyka D, Konat Ł. Case study of accelerated wear of brake discs made of grey cast iron characterized by increased thermal stability. Combustion Engines. 2022;190(3):45-49. https://doi.org/10.19206/CE-146698
[18] Worsztynowicz B, Uhryński A. The analysis of heating process of catalytic converter using thermo-vision. Combustion Engines. 2015;162(3):41-51. https://doi.org/10.19206/CE-116864
[19] Worsztynowicz B, Uhryński A, Borkowski B, Pluta M. The analysis of thermal state of catalytic converter depending on fuel supply and engine load using thermo-vision. Combustion Engines. 2017;170(3):30-36. https://doi.org/10.19206/CE-2017-305
[20] Zhu H, Lian S, Jin M, Wang Y, Yang S, Lu Q et al. Review of research on the influence of vibration and thermal fatigue crack of brake disc on rail vehicles. Eng Fail Anal. 2023; 153:107603. https://doi.org/10.1016/j.engfailanal.2023.107603

Prof. Wojciech Sawczuk, DSc., DEng. – Faculty of Civil and Transport Engineering, Poznan University of Technology, Poznan, Poland.
e-mail: *wojciech.sawczuk@put.poznan.pl*

Dipl.-Ing. Armando Miguel Rilo Cañás – Faculty of Civil and Transport Engineering, Doctoral School of Poznan University of Technology, Poznan, Poland.
e-mail: *armando.rilocanas@doctorate.put.poznan.pl*

Sławomir Kołodziejski, MEng. – Faculty of Civil and Transport Engineering, Doctoral School of Poznan University of Technology, Poznan, Poland.
e-mail:
slawomir.kolodziejski@doctorate.put.poznan.pl